Frequency-Selective Transmission by a Leaky Parallel-Plate-Like Waveguide

Ruey Bing Hwang, *Member, IEEE,* and Cherng Chyi Hsiao

***Abstract*—The phenomena of high frequency-selective transmission of a plane wave by a dielectric two-dimensional (2-D) periodic waveguide, comprising a uniform dielectric layer sandwiched by two finite thickness 2-D periodic structures served as the waveguide wall is described. This structure is termed a *leaky parallel-plate-like waveguide* because the waveguide walls are not perfect reflection mirrors. The scattering characteristics and dispersion relation, including the phase and attenuation constants, of the 2-D periodic waveguide are thoroughly analyzed with the modal transmission-line method and Floquet theory. The extraordinary open stopbands caused by the contra-flow coupling between a leaky parallel-plate-like waveguide and the leaky waves, which are generated by 2-D periodic structures (waveguide walls), are displayed in the form of the Brillouin diagram. The phase-match condition is used to verify the resonant coupling between the incident plane wave and the *leaky parallel-plate-like waveguide* modes. Specifically, the transmission peak frequencies are accurately predicted.**

***Index Terms*—Frequency selective structure (FSS), leaky parallel-plate-like waveguide, resonant coupling, two-dimensional (2-D) periodic structures.**

I. Introduction

FREQUENCY selective surface (FSS) has been extensively studied for many years. FSS is generally categorized as metallic FSS typically consisting of many thin conducting elements printed on a dielectric substrate for support [1]–[12], and the dielectric waveguide gratings with periodic variation on its permittivity or permeability [13]–[18]. The total reflection and transmission frequencies of the periodic dielectric layer were accurately estimated from the surface-wave dispersion relation by the average dielectric constant of the one-dimensional (1-D) periodic layer [13]. Resonant scattering from multilayered dielectric gratings has been investigated using the modal transmission line method [14]. A frequency-selective structure based on guided-mode resonance effects in all-dielectric waveguide grating has been demonstrated theoretically and verified experimentally [15]. A recent study analyzed the scattering and guiding characteristics of a dielectric FSS using a full-wave analysis based on a vectorial modal method [16]. Additionally, the dielectric frequency-selective structures consisting of photonic crystals with point or line defects were also applied as Fabry–Perot resonators [19]–[21]. The electromagnetic band-gap (EBG) superstrates including two-dimensional (2-D) periodic structures and controllable defects for a class of patch antennas were adopted as spatial angular filters [22].

The numerical methods for resolving scattering- and guiding-characteristics, and the electromagnetic fields with the 2-D periodic structures have been well developed. To mention a few, these methods include modal transmission line [23]–[27], generalized scattering matrix [28], lattice-sum for 2-D cylinders array [29], finite-difference time domain [30] and finite-element frequency (and time) domain methods [31], [32].

Concerning the phenomena of frequency-selective transmission with the periodic structures [13]–[16], they were based on the phase-match condition between the incident plane wave and the leaky wave with first-order space harmonic. Namely, a plane wave will couple to the space harmonic, and through it excite the waveguide mode. Once excited, this mode will reradiate plane wave into the air region through the same space harmonic, thereby acting as a leaky wave.

This investigation presents a dielectric frequency-selective transmission structure including a *leaky parallel-plate-like waveguide*. The structure under consideration consisted of a uniform guiding layer sandwiched by two finite 2-D periodic structures as its sidewalls. The structure was named a leaky parallel-plate-like waveguide because that the reflection mirrors (2-D periodic structures) were not perfect. Besides, this structure also supports the surface- and leaky- waves and their corresponding space harmonics. We found that the leaky-waves with space harmonics $n = -1$ are responsible for the higher cutoff frequency of the leaky parallel-plate waveguide mode. This structure enables energy to leak away from the waveguide into air. According to the reciprocal theorem, the leaky wave mechanism is the same for receiving and transmitting. The same concept was applied in designing grating couplers acting as a beam-to-surface wave coupling device [23], [24].

This investigation studies the wave phenomena in such a 2-D periodic waveguide in order to clarify the physical picture of wave processes involved in the structure. Specifically, the relationship between the scattering and guiding characteristics of the 2-D periodic waveguide was carefully examined to accurately predict the peak frequencies of transmission, rather than observing frequency-selective transmission.

The dielectric frequency-selective structure can be regarded as a stack of 1-D periodic layers. The Floquet theory and modal transmission-line method [23]–[25] was used to formulate the electromagnetic boundary-value problem as a transmission-line network, thus obtaining the transfer matrix (or generalized scattering matrix) of each 1-D periodic layer. Moreover, the building block (module) scheme, popular in microwave engineering, was

Manuscript received December 8, 2004; revised August 25, 2005. This work was supported by the National Science Council of the Republic of China, Taiwan, under Contract NSC 94-2213-E-009-069.

The authors are with the Department of Communication Engineering, National Chiao Tung University, 1001 Hsinchu, Taiwan, R.O.C. (e-mail: raybeam@mail.nctu.edu.tw).

Digital Object Identifier 10.1109/TAP.2005.861535

used to systematically analyze its scattering and guiding characteristics. Each 1-D periodic (or uniform) layer was taken as a module in the mathematical analysis procedures. Upon determining the input-output relation of each 1-D periodic layer, the response of the overall structure can be immediately obtained by cascading these building blocks.

Extensive numerical calculations were performed based on the theory described previously. Specifically, the scattering characteristics of the 2-D periodic structures were analyzed to observe the phenomena of frequency-selective transmission. Additionally, the dispersion relation of the 2-D periodic waveguide was rigorously calculated to observe its leaky-wave phenomena. The phase-match condition was applied to identify the resonant coupling between the incident plane wave and *leaky parallel-plate-like mode*. Bertoni, Cheo, and Tamir [13] successfully used this approach to estimate the total reflection and transmission frequencies in the 1-D periodic layer. Furthermore, the frequency-selective transmission frequency was correctly predicted using the rigorous dispersion relation. Additionally, the quality factor of the 2-D periodic waveguide was calculated to qualitatively predict the transmission bandwidth.

The rest of this paper is organized as follows. Section II describes the geometric structure and incident condition with the problem under consideration. Section III outlines the mathematical analysis procedure. Section IV includes extensive numerical examples to examine the frequency-selective transmission. Furthermore, the dispersion relation, including the phase and attenuation constants, was calculated rigorously by transverse resonance. The phase-match condition was used to verify the resonant coupling. Conclusions are finally drawn in Section VII.

II. Problem Statement

The dielectric frequency-selective structure consists of a stack of 1-D periodic layers and uniform dielectric separators, as displayed in Fig. 1(a). This structure can be regarded as a uniform guiding layer sandwiched by two 2-D periodic structures. Half of the structure was redrawn as shown in Fig. 1(b). The thickness of the half uniform guiding layer is given by h, and the relative dielectric constant is assumed to be ε_u. The 2-D periodic structure can be treated as a stack of 1-D periodic layers. For instance, the 2-D periodic structure contains five 1-D periodic layers, as shown in Fig. 1(b). Each 1-D periodic layer is composed of two dielectric media with dielectric constants ε_1 and ε_2 and widths d_1 and d_2. The thickness of the 1-D periodic layer is given by t_p. The dielectric separator between two 1-D periodic layers is denoted as ε_s, and the width is given by t_s. The periods along the x and z directions are given by $d_x(= d_1 + d_2)$ and $d_z(= t_p + t_s)$, respectively. The uniform layer in the middle can be regarded as a *defect* in the width or constituent medium of a complete 2-D periodic structure. Significantly, this structure converges into a 2-D periodic structure if the thickness of the uniform layer $2h = t_s$ and $\varepsilon_u = \varepsilon_s$.

The fields and structure were assumed not to vary along the y direction. Therefore, the overall problem can be separately treated as a scalar electromagnetic boundary-value problem with TE(E_y) or TM(H_y) polarization. A plane wave is obliquely incident from the input region, designated as air, with an incident angle $\theta_{\rm inc}$.

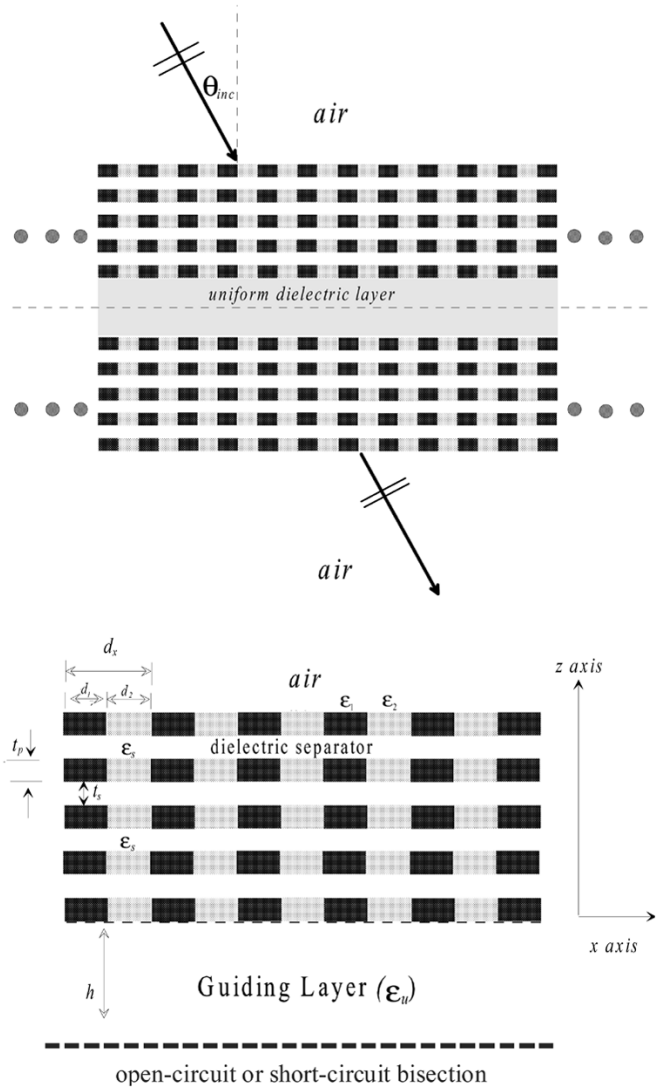

Fig. 1. Structure configuration: (a) dielectric frequency-selective structure consisting of a uniform guiding layer (thickness is $2h$) sandwiched by two finite 2-D periodic structures, and (b) half of the structure with open-circuit or short-circuit bisection.

Besides the scattering problem, the dispersion relation of waves, such as the surface waves and leaky waves, in such a 2-D periodic structure were also computed. The structure can be considered as open-circuit bisection (OCBS) and short-circuit bisection (SCBS) bisections owing to the symmetry of the structure along the z direction, as revealed in Fig. 1(b). Thus, only half of the structure with open-circuit or short-circuit termination need be considered, reducing the complexity of mathematical calculations.

III. Method of Analysis

The structure under consideration was a cascade of multiple 1-D periodic layers, as shown in Fig. 1. The electric and magnetic fields in each 1-D periodic layer were expressed in terms of the Floquet solutions, and the periodic medium was expanded

by the Fourier series expansion. By imposing the electromagnetic boundary conditions at the interface between two adjacent layers, the input-output relation of the discontinuity could be obtained, yielding the input-output relation (transfer matrix) of a 1-D periodic layer. Notably, the uniform layer could be treated as a 1-D periodic layer with vanishing periodic variation, and thus its input-output relation can also be expressed similarly to that of a 1-D periodic layer. Furthermore, the scattering characteristics of the overall structure were determined by cascading these transfer matrices. Two schemes, the scattering of plane waves by the structure and the dispersion relation of waves guided in the structure, were used to analyze this problem. The detailed mathematical procedures regarding in these two schemes were developed and could be found in literature [23]–[27]. In this paper, we merely list some important equations for easy reference.

The periodic structure is assumed to extends infinitely along the x direction. Thus, the dielectric constant of the medium can be expressed as

$$\varepsilon(x + d_x) = \varepsilon(x). \tag{1}$$

Such a periodic dielectric function can be expanded with the Fourier series expansion, which yields

$$\varepsilon(x) = \sum_{n=-\infty}^{n=+\infty} \varepsilon_n \exp\left(-jn\frac{2\pi}{d_x}x\right). \tag{2}$$

With periodic variation, the tangential components of electric and magnetic fields in a 1-D periodic layer are expressed as

$$E_t^{(i)}(x,z) = \sum_n \sum_m q_{n,i}^{(m)} \left(e^{-jk_{zm}^{(i)}z} f_m^{(i)} + e^{+jk_{zm}^{(i)}z} g_m^{(i)}\right) \times e^{-jk_{xn}x} \tag{3a}$$

$$H_t^{(i)}(x,z) = \sum_n \sum_m p_{n,i}^{(m)} \left(e^{-jk_{zm}^{(i)}z} f_m^{(i)} - e^{+jk_{zm}^{(i)}z} g_m^{(i)}\right) \times e^{-jk_{xn}x} \tag{3b}$$

with $k_{xn} = k_{xo} + n(2\pi/d_x)$. The index i represents the ith 1-D periodic layer where k_{xo} denotes the propagation constant along the x direction, which is given by the incident condition when processing the scattering analysis, but is an unknown in the dispersion relation calculation.

Subscript t with the electric and magnetic fields in (3) represents the tangential component. Specifically, the field components are (E_y, H_x) for TE polarization, and (H_y, E_x) for TM polarization, respectively. The integer n denotes the space harmonic index, which ranges from negative to positive infinity.

The parameter $k_{zm}^{(i)}$ denotes the propagation constant along the z direction, which is obtained by solving an eigenvalue problem [17]. The parameters $p_{n,i}^{(m)}$ and $q_{n,i}^{(m)}$ are the components of the eigenvector associated with the eigenvalue. The unknown coefficients $f_m^{(i)}$ and $g_m^{(i)}$ denote the amplitudes of the modes (eigen-functions) propagating along the positive- and negative-z directions, respectively, which were determined once the incident condition was specified. Additionally, the periodic variation of the uniform dielectric layer is assumed to disappear. Thus, the tangential electric and magnetic fields share a similar form as given in (3).

Moreover, the input-output relation of a 1-D periodic (or uniform) layer could be written as

$$\underline{E}_t(z = l) = \mathbf{T}\underline{E}_t(z = o) \tag{4}$$

where the parameters $z = o$ and $z = l$ represent the positions of the two interfaces of the 1-D periodic layer. Where the vector $\underline{E}_t$ is a vector with its components representing the voltage amplitude of each space harmonic. The full matrix $\mathbf{T}$ denotes the transfer matrix, relating the electric field at the two interfaces of a 1-D periodic (or uniform) layer. A detailed formulation and mathematical procedure can be found in [23]–[27].

On determining the transfer matrix of each 1-D periodic layer, the scattering characteristics of the overall structure, comprising multiple 1-D periodic layers, can be further calculated by cascading those transfer matrices. In doing so, the reflectance and transmittance of each space harmonic are obtained as the incident plane wave is given. Additionally, the dispersion relation of the source-free fields supported by the structure can be obtained using transverse resonance technique [14]. In this case, the dispersion root k_x, is generally a complex root, with its real and imaginary parts denoting the phase and attenuation constants along the x direction.

IV. Verification of the Computer Program

Before extensive numerical calculations are performed, the plane wave scattering by a 2-D periodic structure containing cylindrical dielectric rods arrays [32] (relative dielectric constant $\varepsilon_r = 4.2$, diameter is 4 mm, the period is 9 mm, and incident angle is 50°) was calculated to verify the accuracy of the proposed computer program. We employed the staircase approach to partition the circular cylinders into many very fine rectangular slices. Thus, the mathematical formulation procedures described in the Section III are still available. We have carried out the convergence test for the transmittance response against the number of partitions for ensuring the accuracy of the results. For each row of the circular cylinder array, we partitioned it into 50 rectangular slices. In doing so, the permittivity inside every layer can be assumed to vary in a simple step-wise manner with respect to the z-axis. Fig. 2 illustrates the variation of transmitted power against the operation frequency. A good agreement was found among the four approaches, even up to the high frequency range (for the frequency around 18.9 GHz, the result of this investigation agrees with that of the FEM-nonorthogonal method).

V. Numerical Investigation of the Frequency Selective Transmission for 2-D Periodic Structures

A. Example of Calculations

A computer program was written to compute the scattering characteristics and the dispersion relation of the source-free fields supported by the structure. The parametric studies for the thickness of the uniform layer and the incident angle of plane wave were conducted to observe the variations on the transmittance response. Additionally, the dispersion relations of waveguide modes in the uniform guiding layer were rigorously computed. Moreover, the phase-match between the incident

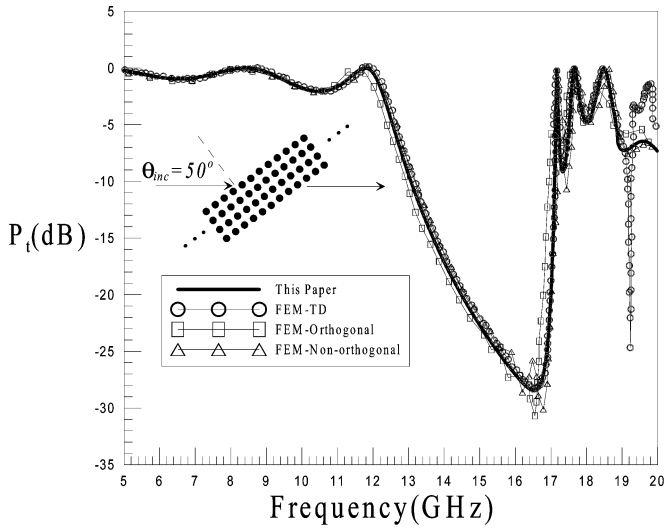

Fig. 2. Variation of transmitted power against frequency for a 4-layer circular dielectric cylinders array incident by a plane wave with an oblique incident angle.

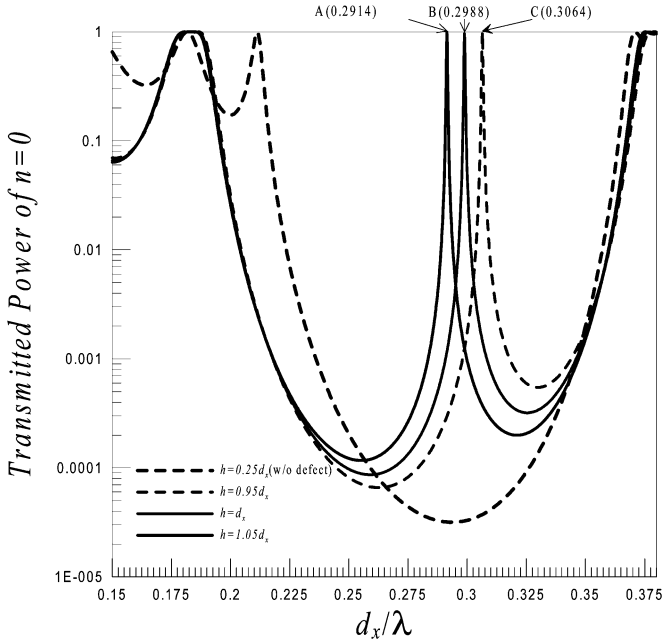

Fig. 3. Variation of the transmittance against normalized frequency for the dielectric frequency selective structure including three 1-D periodic layers on the top and bottom surfaces of the uniform dielectric layer; widths of uniform dielectric layer are: $h = 0.25d_x, 0.95d_x, 1.0d_x, 1.05d_x$.

plane wave and leaky-wave supported by this waveguide is displayed herein to interpret the resonance coupling.

The structure parameters used in the numerical examples throughout this study are given below. The relative dielectric constants of the 1-D periodic layer are: $\varepsilon_1 = 10.2$ and $\varepsilon_2 = 1.03$. The uniform guiding layer has the same relative dielectric constant as the dielectric separator, with $\varepsilon_s = \varepsilon_u = 1.03$. The periods along the x and z directions are the same ($d_x = d_z = d$). The duty cycles of the two dielectric medium in a 1-D periodic layer is 50%. The thicknesses of the 1-D periodic and dielectric separator layers are both $0.5d$. Significantly, all the lengths in this work were normalized to the period d. The top and bottom surface of the uniform dielectric layer both have three 1-D periodic layers.

Fig. 3 displays the variation of the transmittance against the normalized frequency (d_x/λ) for various thicknesses of the uniform dielectric layer. Herein, we kept d_x and iterated the wavelength (λ). This structure includes three 1-D periodic layers on the top and bottom of the dielectric layer. The incident angle of the plane wave is $\theta_{\rm inc} = 44.43°$. Notably, $h = 0.25d_x$ corresponds to a complete 2-D periodic structure comprising six 1-D periodic layers. A significant stopband is present around the normalized frequency $d_x/\lambda = 0.3$. Specifically, a narrow pass band occurs when the thickness h was altered. Such a passband has an excellent frequency-selectivity because it is located in a stopband region. Additionally, the peak frequencies of total transmission for each case were recorded in parentheses for further comparison.

B. Band Structure of the 2-D Periodic Medium

This band structure is similar to a parallel-plate resonator, as showed in the transmission response in Fig. 3. Therefore, the 2-D periodic structures acted as reflection mirrors to maintain the resonator. To inspect the reflection characteristics of the reflection mirrors, the band structure of the 2-D periodic structure must be understood for allocating the frequency range of stopband, where the reflection mirror operates. The following example not only demonstrates the band structure of a 2-D periodic structure with the parameters described previously, but also provides a criterion for choosing the structure parameters.

The 2-D periodic medium can be treated as a stack of 1-D periodic layers. Therefore, the Bloch (periodic) condition was imposed on a unit cell including a 1-D periodic layer plus a uniform dielectric separator [27]. A dispersion relation of waves propagating in a 2-D periodic medium of infinite extent, which defines the relationship among k_o, k_x, and k_z, can thus be obtained. The horizontal axis is the normalized phase constant along the x direction (k_x/k_o), while the vertical axis denotes the normalized frequency (d_x/λ), as indicated in Fig. 4. The zone drawn in black color denotes the pass band region, in which the wave is propagating and the phase constant (k_z/k_o) is a real number. The white zone, otherwise known as the stopband area, possesses a complex propagation constant exhibiting a strong reflection for the waves. The normalized frequency d_x/λ between 0.2 and 0.3 has a complete stop band. Significantly, the normalized phase constant (k_x/k_o) is less than unity enabling this 2-D periodic structure to be used as a reflection mirror within this stopband region.

The band structure for TM polarization was also calculated. The stopband region of TE polarization conversely possessed a passband behavior with TM polarization, although not shown here.

Fig. 5 depicts the variation of transmittance of fundamental space harmonic against the normalized frequency for various incident angles. The structure configuration and parameters under consideration were described in Section V-A. Additionally, the half width of the guiding layer is $h = d_x$. Herein, we kept d_x and iterated the wavelength (λ). The incident angle was changed from 0° to 50° in a 10° increment to observe the variation on the transmitted peak frequency. The six transmission peaks are

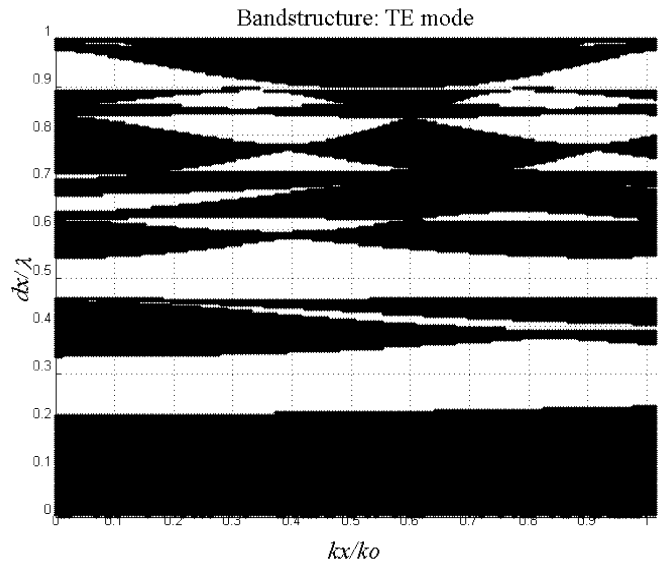

Fig. 4. Band structure of a 2-D periodic medium of infinite extent, the period along x and z axes are both d_x; the duty cycle in both axes are 50%, and the regions drawn in black and white colors denote the passband and stopband areas, respectively.

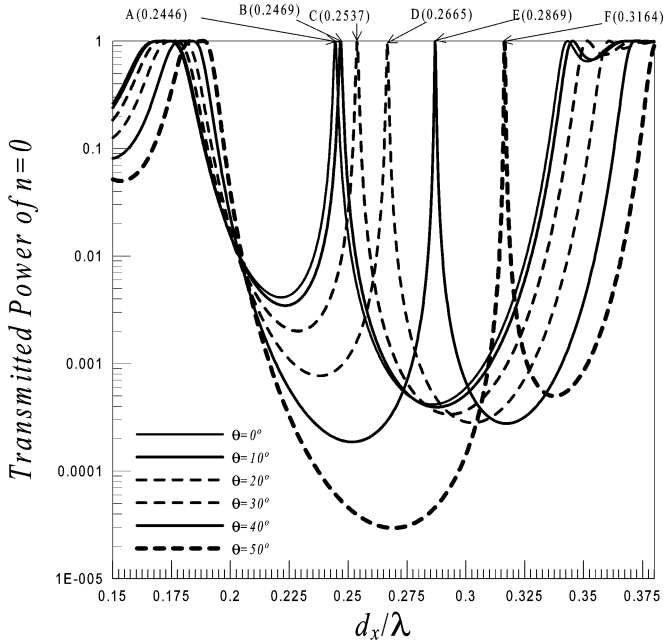

Fig. 5. Variation of the transmittance against normalized frequency for various incident angles θ, with $h = 1.0\,d_x$ and TE polarization.

labeled in alphabetical order and their normalized frequencies are given in round brackets. The increase in the incident angle was found to cause the transmission peak to shift toward higher frequency range, as revealed in Fig. 5. The increase in the transmittance-peak frequency is not linear. Besides, the transmission bandwidth changed as the incident angle was altered. Specifically, the case with larger incident angle has a narrower bandwidth. Moreover, the transmission-peak frequency can be accurately predicted, and the tendency for the change with the bandwidth can be qualitatively interpreted by computing the dispersion relation of such a wave-guiding structure. The transmission response with TM plane wave incidence was also calculated. However, these results are not shown since no

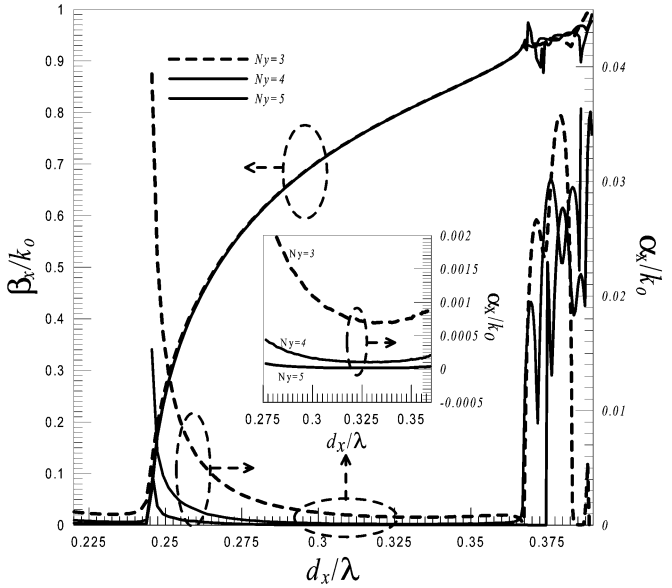

Fig. 6. Dispersion relation of waveguide for various numbers of 1-D periodic layers, open-circuit bisection case with the uniform dielectric layer thickness $h = d_x$.

frequency-selective transmissions for various incident angles were found. It is because that the stop band (total reflection) was not present for the reflection mirrors (2-D periodic structure) with TM polarization fields.

C. Dispersion Relation of the Leaky Parallel-Plate-Like Waveguide

Fig. 6 illustrates the dispersion relation of the parallel-plate-like waveguide for various numbers of 1-D periodic layers, under open-circuit bisection (OCBS). Here, the dispersion root is generally a complex number with its real and imaginary terms denoting the phase (β_x) and attenuation (leaky) constants (α_x), respectively. The number of 1-D periodic layers was altered from 3 to 5 to observe their variation. Notably, the imaginary part (α_x) is mainly caused by the power leakage from the waveguide, since all the dielectric media were assumed to be lossless. The attenuation constant appears to be large and varies rapidly when the normalized frequency is below $d_x/\lambda = 0.24$. Furthermore, the normalized phase constant decreased toward zero as the number of periodic layer increased. The cutoff phenomenon shows that the 2-D periodic structure functions as a reflection mirror. The attenuation constant significantly increased as the normalized frequency exceeded $d_x/\lambda = 0.368$, due to the open stopband (a stopband in the fast-wave region) resulting from coupling between leaky wave and the leaky parallel-plate waveguide mode. The next example clearly explains the coupling using the Brillouin diagram.

Between these two normalized frequencies ($d_x/\lambda = 0.24$ and 0.368), the normalized attenuation constants are insignificant for all three cases. The inset of Fig. 6 shows this region in a magnified form for easy reference. The normalized attenuation constant generally fell as the number of 1-D periodic layers rose. The rise in the thickness of the 2-D periodic structures (waveguide walls) lowered its attenuation constant, as was confirmed by intuition. Additionally, such a *band limited* waveguide

has both lower and upper cutoff frequencies. Below the lower cutoff frequency the wave is evanescent, while above the higher cutoff frequency the wave experiences a strong reflection. Consequently, this waveguide, unlike the traditional dielectric waveguide or metal waveguide, possesses limited bandwidth.

D. Brillouin Diagram of the Leaky Parallel-Plate-Like Waveguide

To study the open stopband in the previous example, the dispersion relation was redrawn as displayed in Fig. 6 with the case of three 1-D periodic layers, in terms of the Brillouin diagram.

This structure inherently contains two types of leaky wave; one is termed the leaky parallel-plate-like waveguide modes, as substantially explained in the previous examples, while the other is the well known leaky wave due to the reflection mirrors (a stack of 1-D periodic layers). The leaky wave wave-numbers can be predicted by considering surface waves associated with a layered medium composed of a stack of homogeneous layers (separator and averaged 1-D periodic layers). When the ratio of period to wavelength (d_x/λ) is sufficiently small, all the space harmonics are evanescent in the open region. If this surface-wave condition is not satisfied, then at least one space harmonic must leak power into the air region. Consequently, the introduction of the periodicity causes the presence of leaky space harmonics. The bound surface wave was modified into the leaky wave possessing a complex propagation constant.

From the literature [13], we know that the dispersion curve of the $n = -1$ space harmonic could be estimated from solving the dispersion relation of a stack of uniform layers, where the 1-D periodic layer was approximated by a uniform dielectric constant equal to the average value in the 1-D periodic layer, if the modulation index (or dielectric contrast) is small enough. However, the dielectric contrast ($\varepsilon_1 = 10.2$ and $\varepsilon_2 = 1.03$) is significant in our numerical example. The results obtained from the small perturbation analysis are not accurate. We have to resort to the rigorous formulation described in Section III to determine the propagation constants.

Notably, all the dispersion curves shown in this figure were obtained by the same mathematical procedure described in Section III. The area in shadow pattern denotes the bound-wave region, while outside it is the fast-wave region, as was shown in Fig. 7. The dispersion curves (for example, the six curves in this figure) in this region are surface waves and their space harmonics, with their normalized phase constant (β_x/k_o) greater than unity. The zone that separates the two groups of dispersion curves is the surface-wave stopband, where the surface waves can not propagate. Moreover, the curves in the fast-wave region, extending from the surface waves in the bound-wave region, are leaky waves. The two dispersion curves circled by a dashed rectangle represent leaky parallel-plate-like waveguide modes, where the lower curve corresponds to that displayed in Fig. 6. The dispersion curves of the leaky parallel-plate-like waveguide modes apparently intersected the leaky waves of space harmonic $n = -1$. The contra-flow coupling in the vicinity of intersection leads to a stopband. Moreover, the stop bands consist of two individual stop bands because the leaky parallel-plate-like waveguide modes coupled with two leaky waves of space harmonic $n = -1$, as depicted in the region denoted by a dashed circle.

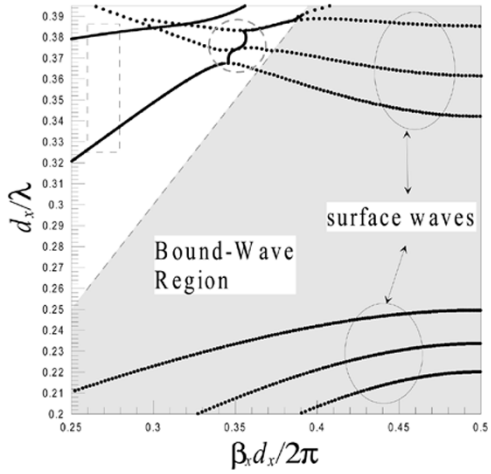

Fig. 7. Brillouin diagram for the periodic waveguide shown in Fig. 1(b) with open-circuit bisection ($h = d_x$). The region marked with a dashed circle is an open stopband. The two curves circled by a dashed rectangle denote leaky parallel-plate-like waveguide modes.

Significantly, such an open (or leaky wave) stop band occurs only in the present structure with periodicity along the x direction. If the periodicity along the x direction disappears, that is, the 1-D periodic layers are replaced by uniform layers, no contra-flow coupling arises since no $n = -1$ leaky wave is excited in this structure.

VI. Predict the Transmission Peak Frequency by the Dispersion Relation of the Waveguide

A. Phase-Match Condition

As we have known, when a plane wave, which can be considered as an excitation, is incident on a leaky waveguide, the structure response is strong when the phase-match condition is satisfied. In this sense the incident plane wave will couple to the waveguide and excite the waveguide mode. Once excited, the mode will reradiate into the open region. Such a coupling mechanism physically interprets the phenomenon of frequency-selective transmission and also provides us a way to predict the transmission frequency.

To demonstrate the phase-match condition, the dispersion curve of the case with three 1-D periodic layers, shown in Fig. 6, was redrawn in Fig. 8, together with the phase constant distribution of the incident plane wave. The horizontal axis is the normalized frequency (d_x/λ). The vertical axes are the normalized propagation constant, with the left-hand axis denoting the phase constant (β_x/k_o) and the attenuation constant (α_x/k_o) at the right-hand side. A plane wave with incident angle θ is obliquely incident on the waveguide, while the normalized phase constant along the x direction is $\beta_x/k_o = \sin\theta$. The dashed lines in this figure show the normalized phase constants of the plane wave with incident angle θ ranging from 10° to 50° with 10° increment. The intersection points reveal the phase matching between the incident plane wave and the guided modes of the waveguide. The number in parentheses after each character are the normalized frequencies at the intersection point, which agree very well with those transmission peak frequencies displayed in Fig. 4. However, the normalized frequency of the transmission peak cannot be predicted in the normal incident case, the

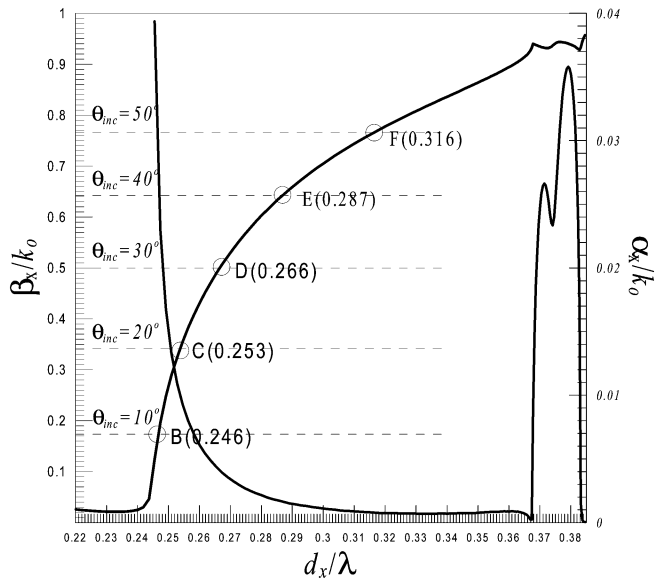

Fig. 8. Distribution of normalized phase and attenuation constants against the normalized frequency; open-circuit bisection case with TE polarization; the black curve denotes the phase constant; the gay curve denotes the attenuation constant; the number of 1-D periodic layer is 3, and $h = d_x$.

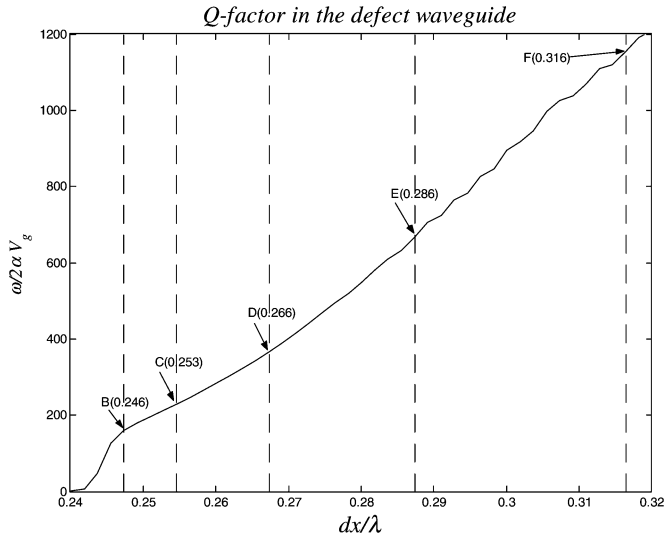

Fig. 9. Variation of the quality-factor against the normalized frequency for the frequency-selective structure with three 1-D periodic layers; $h = 1.0d_x$, OCBS.

phase-match condition is absent due to the lack of an intersection point. Reciprocally, a single leaky mode does not radiate exactly at the broadside with an infinite periodic waveguide, due to its extremely large attenuation constant [33], [35]. Therefore, the transmission peak frequency was estimated roughly by the cutoff condition of the ideal parallel-plate waveguide with width $2h$, which was given as: $d_x/\lambda = d_x/4h\sqrt{\varepsilon_u} = 0.2463$. The dispersion relation of the short-circuit bisection case was also calculated. However, these results are not shown, because this mode did not contribute to the resonant coupling process.

The number of 1-D periodic layer was raised progressively to observe the variations on the dispersion curves and the transmittance response, although the resutls are not displayed in this work. If the number of 1-D periodic layer is increased to 15, the normalized attenuation constant is around 10^{-5}. Besides, the strong reflection occurs and the transmission is insignificant, because that the 2-D periodic structures (waveguide walls) approach ideal reflection mirrors.

Concerning the phase-match condition, the attenuation constant plays an important role in the physical process of wave coupling. The attenuation constant indicates the ability of the waveguide walls to preserve the energy in the waveguide. Namely, the large attenuation constant (for a lossless structure) means that a large amount of power will radiate into the air. Conversely, if the attenuation equals zero, the waveguide is isolated and the wave coupling can not occur. Thus, the frequency-selective transmission can not take place.

B. Quality Factor of the Waveguide

Bandwidth also significantly affects the performance of the frequency selective structure, in addition to the transmission peak frequency. The quality factor of the waveguide should be carefully studied, since the transmission characteristic strongly relates to the resonance coupling. The quality factor of the waveguide was computed with three 1-D periodic layers under the OCBS termination condition. The qualify factor was defined as ($Q = \omega/2\alpha_x v_g$, where ω is the angular frequency; α_x denotes the attenuation, and v_g represents the group velocity) in Collin's text book [34]. This definition is accurate for a dispersive transmission resonator [34]. Significantly, the loss is mainly caused by the radiation (power leakage from the waveguide), since the dielectric media were assumed to be lossless. Furthermore, the quality factor increased with the increase in the normalized frequency, as demonstrated in Fig. 9. Recalling the transmission response in Fig. 5, the transmission bandwidth narrowed as the incident angle increased. This phenomenon indicates that the larger the incident angle, the higher the value of Q.

TABLE I
QUALITY FACTORS EVALUATED USING SEVERAL DEFINITIONS

Q-factor / Samples	$\beta/2\alpha$	$\omega/2\alpha v_g$	Fractional Bandwidth ($f_o/\Delta f$)
B	3.70	174.21	176.18
C	16.94	225.55	216.05
D	60.57	365.53	310.6
E	195.50	662.47	453.65
F	485.25	1144.09	656.68

The quality factor was also calculated by the other two definitions, which are fractional bandwidth definitions $(f_o/\Delta f)$ and $\beta/2\alpha$. The Q-factor values obtained based on the three different definitions are listed in Table I. The quality factor (obtained by evaluating $\omega/2\alpha v_g$) was closer to that obtained from the fractional bandwidth definition than it was to that obtained by the definition $\beta/2\alpha$ for the cases B, C and D, because that the waveguide is considerably dispersive. However, the values with the cases E and F were not consistent among the three definitions. Nevertheless, these three definitions of Q factor have similar tendency of variation.

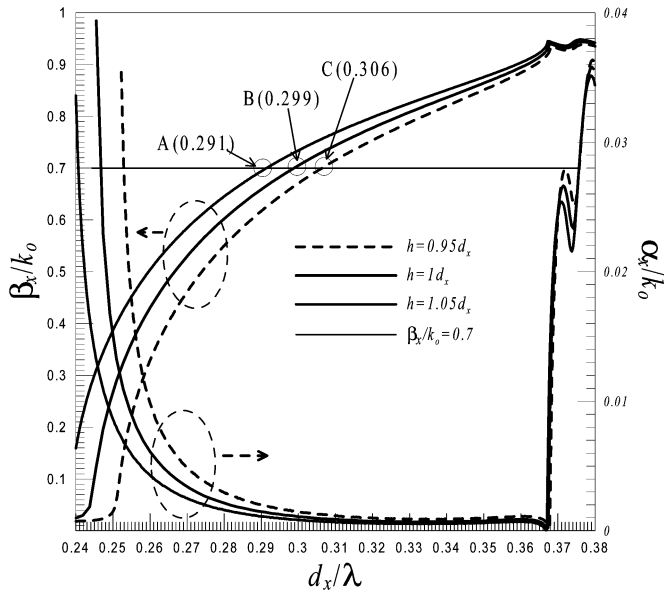

Fig. 10. Dispersion relation of waveguide with channel widths $h = 0.95d_x$, $1.0d_x$ and $1.05d_x$; open-circuit bisection case with TE polarization. The horizontal line is the normalized phase constant of the incident plane wave with oblique incident ($\theta_{\rm inc} = 44.43^\circ$).

C. Variation of the Waveguide Channel Width on the Dispersion Relation and Transmission Peak Frequency

Fig. 10 shows the dispersion relation, including the normalized phase and attenuation constants, of the waveguide with channel widths $h = 0.95d_x$, $1.0d_x$, and $1.05d_x$. The left-hand and right-hand axes denote the normalized phase and attenuation constants, respectively, while the horizontal axis represents the normalized frequency. The dispersion relation of waveguide is similar to that of the metallic parallel-plate waveguide, since the 2-D periodic structure acts as a reflection mirror. Therefore, the phase constant can be approximated using the simple formula:$\beta_x \approx \sqrt{k_o^2\varepsilon_u - (\pi/2h)^2}$. Moreover, the increase in width h leads to an increase in phase constant as the operation frequency is fixed, which is confirmed in Fig. 10. Additionally, the transmittance response in Fig. 3, with the incident condition designated as $\beta_x/k_o = 0.7$ ($\theta_{\rm inc} = 44.43^\circ$), is recalled. Using the phase-match condition, the transmission peak frequency could be correctly predicted from the intersection points denoted by A, B, and C.

VII. Conclusion

This investigation presents the phenomena of high frequency-selective transmission of the structure comprising a uniform dielectric layer sandwiched by two 2-D periodic structures of finite thickness. The band-structure of the waveguide wall (2-D periodic structure) was first calculated. Therefore, the scattering characteristic of the parallel-plate-like waveguide was computed to exhibit the frequency-selective transmission. Additionally, the dispersion elation of such a 2-D periodic waveguide was calculated to observe its wave-guiding phenomena. The resonant coupling, owing to the coupling between the incident plane wave and leaky parallel-plate-like waveguide modes, was systematically verified with a phase-match condition. The Brillouin diagram was utilized to investigate the extraordinary open stopbands resulting from the contra-flow coupling between a leaky parallel-plate-like waveguide and the leaky waves contributed by the 2-D periodic structures (waveguide walls).

Acknowledgment

The authors would like to thank the National Science Council of the Republic of China, Taiwan, for financially supporting this research.

They would also like to thank Prof. S. Tsuen, Peng, Emeritus Professor of National Chiao Tung University, whose mentoring in the area of periodic structures and encouragement in this research is appreciated. The Reviewer's valuable comments are also appreciated.

References

[1] V. D. Agrawal and W. A. Imbriale, "Design of a dichroic cassegrain subreflector," *IEEE Trans. Antennas Propag.*, vol. AP-27, no. 4, pp. 466–473, Jul. 1979.

[2] B. A. Munk, *Frequency Selective Surfaces: Theory and Design*. New York: Wiley, 2000.

[3] ——, *Finite Antenna Arrays and FSS*. New York: Wiley, 2003.

[4] C. V. John, *Frequency Selective Surfaces*, U.K.: Research Studies Press, 1997.

[5] T. K. Wu, *Frequency Selective Surfaces and Grid Array*. New York: Wiley, 1995.

[6] E. L. Pelton and B. A. Munk, "Periodic Antenna Surface of Ttriple Slot Elements," U.S. Patent 3 975 735, Aug. 17, 1976.

[7] S. W. Lee, G. Zarrillo, and C. L. Law, "Simple formulas for transmission through periodic metal grids or plates," *IEEE Trans. Antennas Propag.*, vol. AP-30, no. 5, pp. 904–909, Sep. 1982.

[8] R. Mittra, C. Chan, and T. Cwik, "Techniques for analyzing frequency selective surfaces—A review," *Proc. IEEE*, vol. 76, no. 23, pp. 1593–1615, 1988.

[9] R. H. Ott *et al.*, "Scattering by a two-dimensional periodic array of conducting plates," *Radio Sci.*, vol. 2, no. 11, pp. 1347–1359, 1967.

[10] G. H. Schennum, "Frequency selective surfaces for multiple frequency antennas," *Microwave J.*, vol. 16, no. 5, pp. 55–57, 1973.

[11] R. C. Compoton *et al.*, "Diffraction properties of a bandpass grid," *Infared Phys.*, vol. 23, no. 5, pp. 239–245, 1983.

[12] R. J. Luebbers and B. A. Munk, "Some effects of dielectric loading on periodic slot arrays," *IEEE Trans. Antennas Propag.*, vol. AP-26, no. 4, pp. 536–542, Jul. 1978.

[13] H. L. Bertoni, L.-H. S. Cheo, and T. Tamir, "Frequency-Selective reflection and transmission by a periodic dielectric layer," *IEEE Trans. Antennas Propag.*, vol. AP-37, no. 1, pp. 78–83, Jan. 1989.

[14] T. Tamir and S. Zhang, "Resonant scattering by multilayered dielectric gratings," *J. Opt. Soc. Amer.*, vol. 14, pp. 1607–1616, 1997.

[15] S. Tibuleac, R. Magnusson, T. A. Maldonado, P. P. Young, and T. R. Holzheimer, "Dielectric frequency-selective structures incorporating waveguide gratings," *IEEE Trans. Microwave Theory Tech.*, vol. 48, no. 4, pp. 553–561, Apr. 2000.

[16] A. Coves, B. Gimeno, J. Gil, M. V. Andres, A. A. S. Blas, and V. E. Boria, "Full-Wave analysis of dielectric frequency-selective surfaces using a vectorial modal method," *IEEE Trans. Antennas Propag.*, vol. 52, no. 8, Aug. 2004.

[17] H. Inouye, M. Arakawa, J. Y. Ye, T. Hattori, H. Nakatsuka, and K. Hirao, "Optical properties of a total-reflection-type one-dimensional photonic crystal," *IEEE J. Quantum Electron.*, vol. 38, no. 7, pp. 867–871, Jul. 2002.

[18] J. J. Fratamico *et al.*, "A wide-scan-quasioptical frequency diplexer," *IEEE Trans. Microwave Theory Tech.*, vol. MTT-30, no. 1, pp. 20–27, Jan. 1982.

[19] M. M. Beaky, J. B. Burk, H. O. Everitt, M. A. Haider, and S. Venakides, "Two-Dimensional photonic crystal fabry-perot resonators with lossy dielectrics," *IEEE Trans. Microwave Theory Tech.*, vol. 47, no. 11, pp. 2085–2091, Nov. 1999.

[20] J. Yonekura, M. Ikeda, and T. Baba, "Analysis of finite 2-D photonic crystals of columns and lightwave device using the scattering matrix method," *IEEE J. Lightwave Technol.*, vol. 17, no. 8, pp. 1500–1508, Aug. 1999.

[21] F. Frezza, L. Pajewski, and G. Schettini, "Periodic defects in 2-D-PBG material: Full-wave analysis and design," *IEEE Trans. Nanotechnol.*, vol. 2, no. 3, pp. 126–134, Sep. 2003.
[22] Y. J. Lee, J. Yeo, R. Mittra, and W. S. Park, "Application of electromagnetic bandgap (EBG) superstrates with controllable defects for a class of patch antennas as spatial angular filters," *IEEE Trans. Antennas Propag.*, vol. 53, no. 1, pp. 224–235, Jan. 2005.
[23] S. T. Peng, T. Tamir, and H. L. Bertoni, "Theory of dielectric grating waveguides," *IEEE Trans. Microwave Theory Tech.*, vol. MTT-23, no. 1, pp. 123–133, Jan. 1975.
[24] T. Tamir and S. Zhang, "Modal transmission-line theory of multilayered grating structures," *J. Lightwave Technol.*, vol. 14, pp. 914–927, 1996.
[25] R. E. Collin, "Field theory of guided waves," in *Periodic Structures*, 2nd ed: IEEE Press, 1991, ch. 9.
[26] R. B. Hwang and S. T. Peng, "Scattering and guiding characteristics of waveguides with two-dimesionally periodic walls of finite thickness," *Radio Sci.*, vol. 38, no. 5, pp. 1091–1103, 2003.
[27] R. B. Hwang, "Relations between the reflectance and band structure of 2-D metallodielectric electromagnetic crystals," *IEEE Trans. Antennas Propag.*, vol. 52, no. 6, Jun. 2004.
[28] R. C. Hall, R. Mittra, and K. M. Mitzner, "Analysis of multilayered periodic structures using generalized scattering matrix theory," *IEEE Trans. Antennas Propag.*, vol. 36, no. 4, pp. 511–517, Apr. 1988.
[29] N. A. Nicorovici and R. C. McPhedran, "Lattice sums of off-axis electromagnetic scattering by gratings," *Phys. Rev. E*, vol. 50, pp. 3143–3160, 1994.
[30] D. Maystre, "Electromagnetic study of photonic band gaps," *Pure Appl. Opt.*, vol. 3, pp. 975–993, Nov. 1994.
[31] A. Mekis, S. Fan, and J. D. Joannopoulos, "Absorbing boundary conditions for FDTD simulations of photonic crystal waveguides," *IEEE Microw. Guided Wave Lett.*, vol. 9, pp. 502–504, Dec. 1999.
[32] L. E. R. Petersson and J.-M. Jin, "A two-dimensional time-domain finite element formulation for periodic structure," *IEEE Trans. Antennas Propag.*, vol. 53, no. 4, pp. 1480–1488, Apr. 2005.
[33] M. Guglielmi and D. R. Jackson, "Broadside radiation from periodic leaky-wave antennas," *IEEE Trans. Antennas Propag.*, vol. 41, no. 1, pp. 31–37, Jan. 1993.
[34] R. E. Collin, "Field theory of guided waves," in *Transmission Lines*, 2nd ed: IEEE Press, 1991, ch. 4, pp. 299–299.
[35] R. E. Collin and F. J. Zucker, *Antenna Theory, Part II*. New York: McGraw-Hill, 1969, ch. 19.

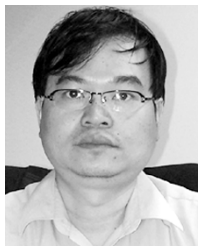

Ruey Bing Hwang (M'96) was born in Nantou, Taiwan, R.O.C., on January 20, 1967. He received the B.S. degree in communication engineering and the Ph.D degree in electronics from National Chiao-Tung University, Hsinchu, Taiwan, R.O.C., in 1990 and 1996, respectively, and the Master degree in electrical engineering from National Taiwan University, Taipei, Taiwan, R.O.C., in 1992.

Following 1996, he joined National Center of High Performance Computing, Hsinchu, as an Associate Research Scientist. From 1999 to 2000, he was a Postdoctoral Research Fellow at National Chiao-Tung University, where, from fall 2000 to spring 2002, he was a Research Associate Professor in the Microelectronics and Information Systems Research Center. From spring 2002 to summer 2004, he was an Associate Professor of the Graduate Institute of Communication Engineering, National Chi Nan University, Nantou, Puli, Taiwan, R.O.C. In August 2004, he joined the faculty of the Department of Communication Engineering, National Chiao Tung University. His research interests include the guiding and scattering characteristics of periodic structures (or photonic crystals), metamaterials, waveguide antennas, array antennas design, and electromagnetic compatibility.

Dr. Hwang is a Member of Phi Tau Phi.

Cherng Chyi Hsiao is working toward the Ph.D. degree at the Department of Communication Engineering, National Chiao Tung University, Hsinchu, Taiwan, R.O.C., under Prof. Hwang's guidance.